# Enhancing sit-to-stand transitions and walking efficiency in older adults with a soft robotic suit

Xiaohui Zhang[†1*], Enrica Tricomi[†1], Marios Stefanakis[2], Nathalie Gierden[1], Theresa Buchner[2], Luka Mišković[1], Jürgen M. Bauer[2,3], Christian Werner[2], Clemens Becker[2,3] and Lorenzo Masia[1]

[1]Department of Computer Engineering, School of Computation, Information and Technology, Technical University of Munich, Munich, Germany.
[2]Geriatric Center, Medical Faculty Heidelberg, Heidelberg University, Heidelberg, Germany.
[3]Network Aging Research, Heidelberg University, Heidelberg, Germany.

*Corresponding author. E-mail: xiaohui.zhang@tum.de;
Contributing authors: † These authors contributed equally to this work;

## SUPPLEMENTARY INFORMATION

### This PDF file includes

- Hardware Components and Locations
- Controller Implementation
- Individual Sit-and-Stand Performance
- Individual Walking Performance
- Individual Gait Smoothness
- Distribution of Sense of Agency Responses

### Other Supplementary Material

- Recorded data and code for analyses
- Video accompanying the paper

## Hardware Components and Locations

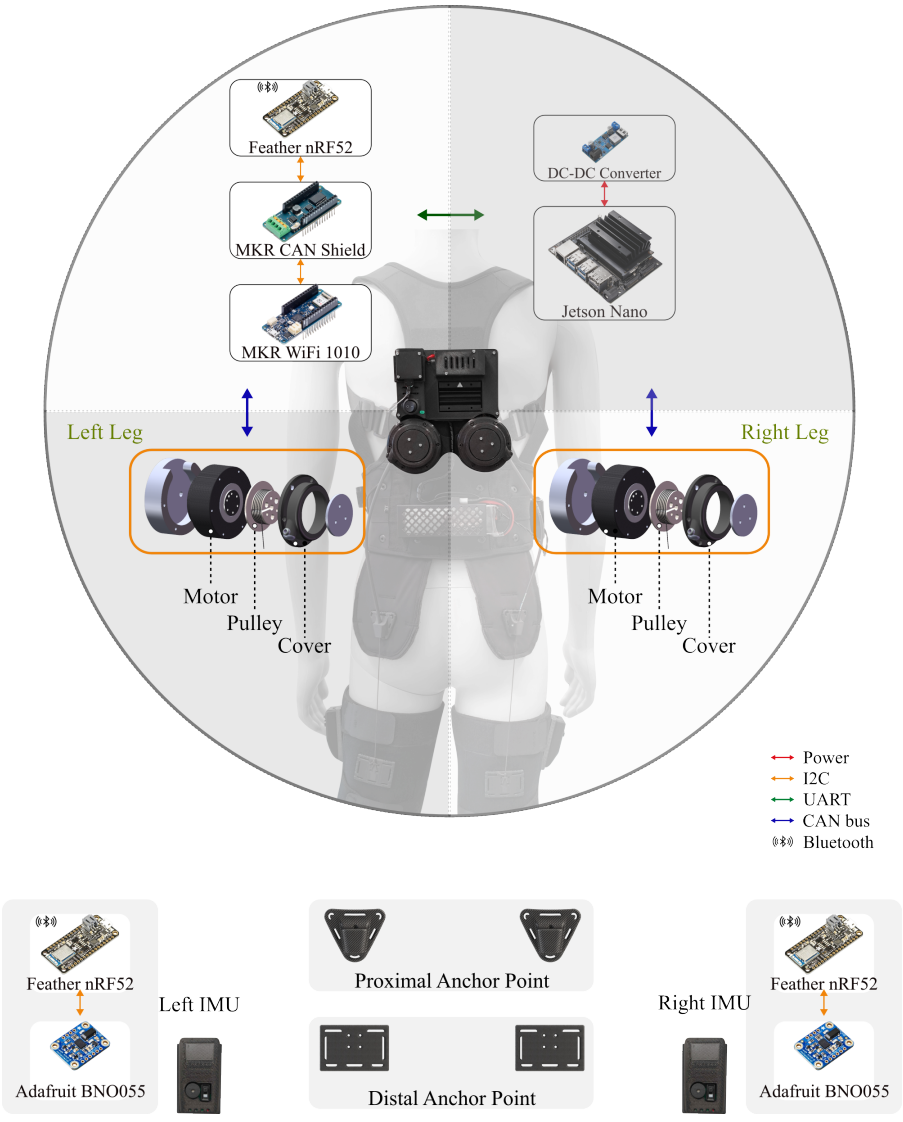


**Fig. S1 Hardware components and locations of the soft wearable exosuit.**

In the soft wearable exosuit, the back-mounted hardware box, together with the left and right IMU units integrates all key electronics. Fig. S1 illustrates

the detailed electronic components within each module. IMU units based on the Adafruit BNO055 (Bosch, BNO055, Germany) are mounted on the left and right thighs to measure the user's hip joint angle and velocity. These kinematic signals are transmitted in real time via Bluetooth from a Feather board (BLE, Feather nRF52 Bluefruit, Adafruit, USA) to a second Feather board located in the upper-left corner of the back hardware enclosure. The signals are then forwarded via the Inter-Integrated Circuit ($I^2C$) bus to an Arduino (MKR 1010 WiFi, Arduino, Italy) equipped with a CAN-bus shield (CAN-bus Shield V2.0, Seeed Studio, China). Finally, the processed data are transmitted in real time to the Jetson Nano (NVIDIA, USA) for locomotion mode detection and gait phase estimation. The Jetson generates motor reference trajectories that are sent back to the Arduino, which drives the actuators via the Can-bus, rotating the motors and the pulleys mounted above them. Rotation of these pulleys tightens and releases the artificial tendons routed to proximal and distal anchor points on each thigh, thereby delivering assistive forces to the user. In addition to the electronic boards, the housings, pulley components, and both proximal and distal anchor points are fabricated by 3D printing technology with PLA (polylactic acid).

# Controller Implementation

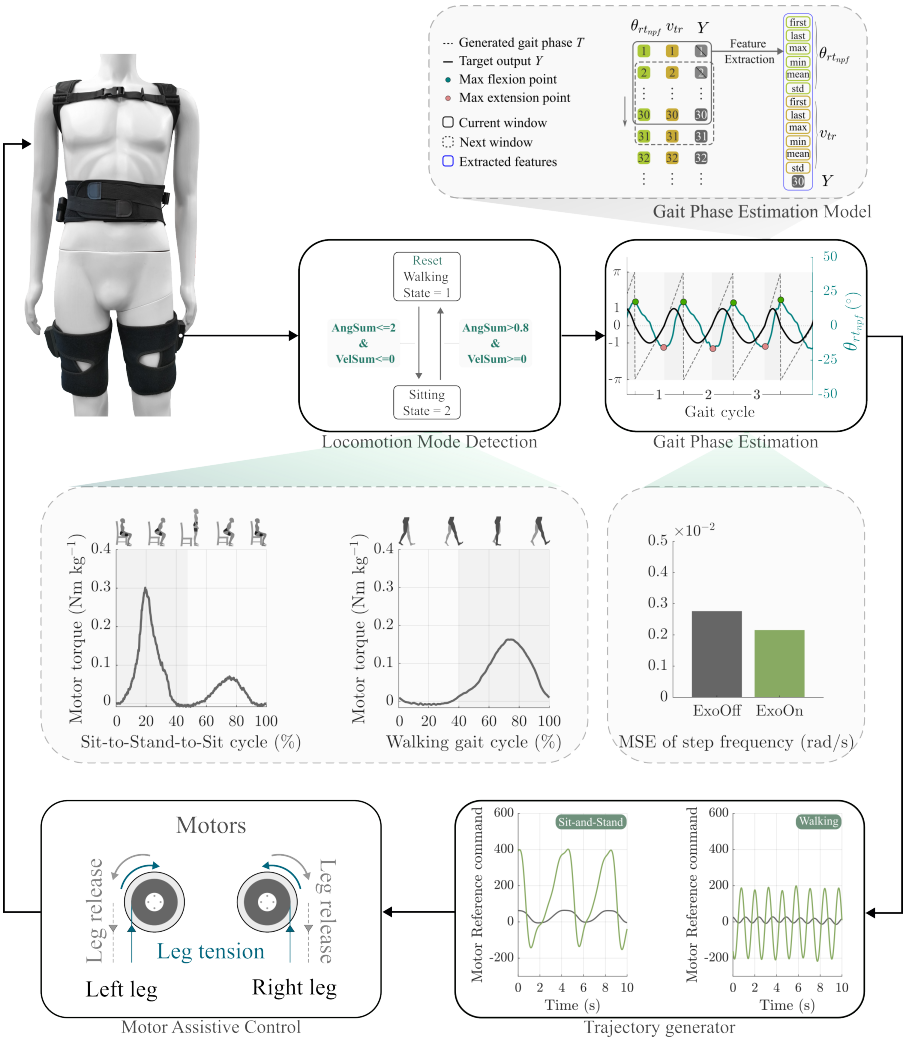


**Fig. S2 Schematic diagram and detailed illustration of the controller's working principle.**

The controller of the exosuit is structured into a high-level and a low-level layer.

## High Level of the Controller

**Locomotion mode detection:** The exosuit provides assistive forces to the user during sit-to-stand transitions and leg extension in walking. Locomotion mode detection of the exosuit is implemented using a finite-state machine that switches between sitting and walking modes based on threshold conditions on the bilateral hip joint angle (AngSum) and velocity (VelSum). Fig. S2 also presents the motor torque profiles from a representative participant during sit-and-stand and overground walking movements. Compared with walking, the magnitude of assistance delivered during sit-to-stand transfers is higher.

**Table S1 Young participants information for training data collection in the gait phase estimation model**

| Participant | Sex (F/M) | Age (year) | Weight (kg) | Height (cm) |
|---|---|---|---|---|
| P1 | M | 24 | 82 | 183 |
| P2 | M | 28 | 69 | 182 |
| P3 | F | 25 | 60 | 166 |
| P4 | M | 28 | 82 | 180 |
| P5 | M | 24 | 68 | 170 |
| P6 | F | 24 | 50 | 164 |
| P7 | M | 27 | 83 | 182 |
| P8 | M | 27 | 85 | 193 |

**Gait phase estimation model:** Eight healthy participants were recruited for data collection for the gait phase estimation model, and their detailed characteristics are summarized in Tab. S1. Each participant completed a 400m walk on level ground at a self-selected speed followed by one minute of quiet standing. Two kinematic signals were selected as input for the gait phase estimation model: the notch-peak filtered angle ($\theta_{rt_{npf}}$) and the angular velocity ($v_{rt}$) of the thigh. These signals reflect key dynamic characteristics throughout the gait cycle and were acquired in real time within a MATLAB/Simulink environment. The output labels for model training were generated through a semi-manual annotation process. As illustrated in Fig. S2, maximum flexion points and maximum extension points were detected from the $\theta_{rt_{npf}}$ signal to

segment individual gait cycles. For each cycle, a continuous gait phase vector $T$ was constructed by linearly interpolating values from $[-\pi, 0]$ between the maximum flexion point and the maximum extension point, and from $[0, \pi]$ between the maximum extension point and the subsequent maximum flexion point. To ensure phase continuity across cycles and avoid discontinuities at transitions, the final target output was defined as $Y = \sin(T + \tau)$, with $\tau \in [0, \pi]$ representing a tunable delay compensation parameter initialized to 0.

Here, we obtained two kinematic input signals and one output label $Y$ to construct the training dataset for the regression model. A sliding window technique was applied to the raw sequential signals to extract gait phase features. At each sliding step (corresponding to one sample interval at a sampling rate of 100 Hz in the MATLAB/Simulink environment), the window captured 30 consecutive samples from each signal channel. For each input signal within the current window (e.g., $\theta_{rt_{npf}}$ and $v_{rt}$), six statistical features were computed: the first value, last value, maximum, minimum, mean, and standard deviation. These features were concatenated across the two channels to form a 12-dimensional input feature vector. The corresponding label for each feature vector was defined as the last value of the gait phase label $Y$ within the same window. The regression model was trained using the *fitrensemble* function in MATLAB/Simulink R2021b, incorporating 30 decision trees with a maximum of 1024 splits each. The final prediction was derived by averaging the outputs of the individual trees.

Since the gait phase estimation model was trained on data from healthy young participants, we evaluated its gait phase estimation performance in older adults by quantifying the mean absolute error (MAE) between the actual and estimated gait frequency during walking across all participants.

The MAE result of gait frequency estimation was less than 0.003 for all participants in both *ExoOff* and *ExoOn* conditions. These results demonstrate the effectiveness of the gait phase estimation model across different age groups.

**Low-Level of the Controller** The trajectory generator uses the estimated gait phase $Y$ from the high-level of the controller to produce appropriate reference trajectories for different locomotion modes. Fig. S2 shows the motor reference trajectories for a representative participant across the different modes. Specifically, in walking mode, the predicted gait phase $Y$ is scaled by a gain factor $k \in [1, 5]$ to generate the target motor trajectory, expressed as $R_{traj} = k * Y$. The scaling factor $k$ can be flexibly adjusted according to the individual user's needs to achieve personalized assistance. In sit-to-stand transitions, the controller enhances actuator responsiveness and vertical support by using the right leg's angular velocity $v_{rt}$ as the control variable to define the reference trajectory as $R_{traj} = 2 * v_{rt}$. To ensure smooth transitions between modes and to avoid abrupt actuator responses, the reference trajectory is passed through a second-order low-pass filter with a cutoff frequency of 4.8 Hz. This filtering effectively attenuates high-frequency noise and ensures the continuity and stability of the generated motion profiles.

The filtered reference trajectory is then tracked by a proportional controller with a first-order low-pass characteristic. This controller converts the error between the desired and actual motor positions into a motor angular velocity command. Its transfer function is given by:

$$H_p(s) = \frac{K_p}{1 + K_d \cdot s} \tag{1}$$

where $K_p = 8$ and $K_d = 0.06$ are experimentally tuned parameters that were found to provide a good balance between fast system response, tracking accuracy, and user comfort.

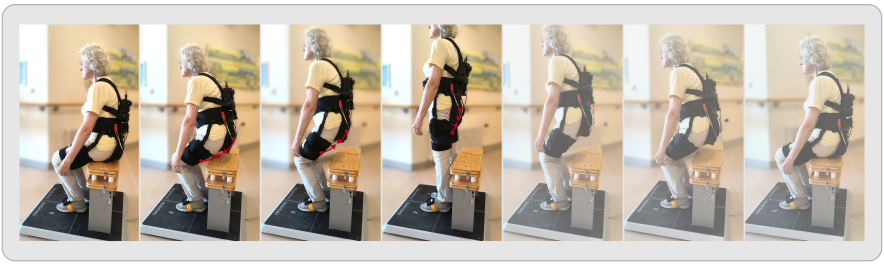

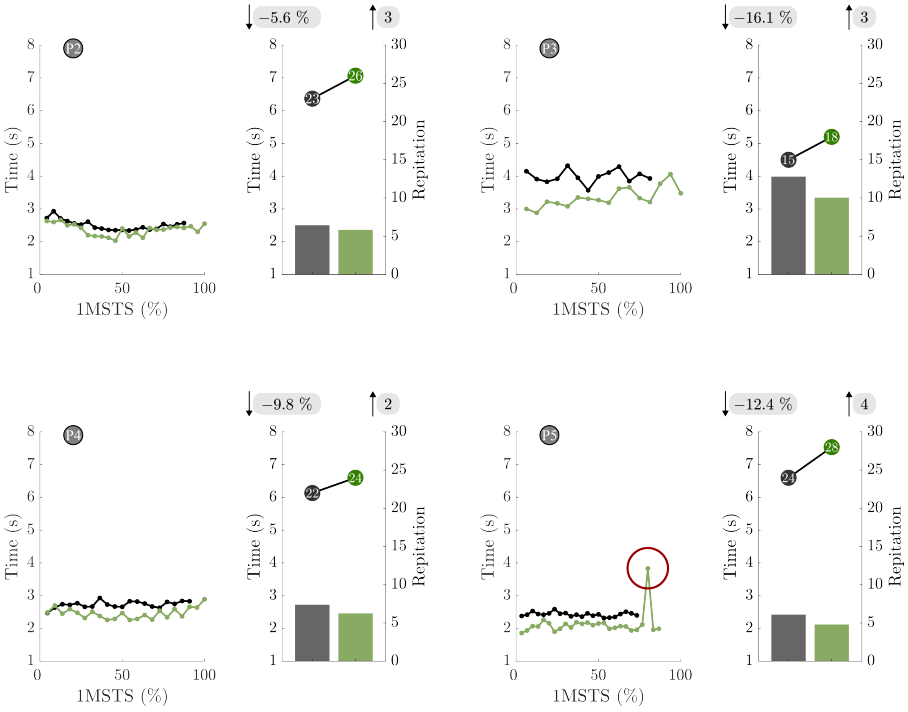
P2
−5.6 %
3
P3
−16.1 %
3
P4
−9.8 %
2
P5
−12.4 %
4
Time (s)
Repitation
1MSTS (%)

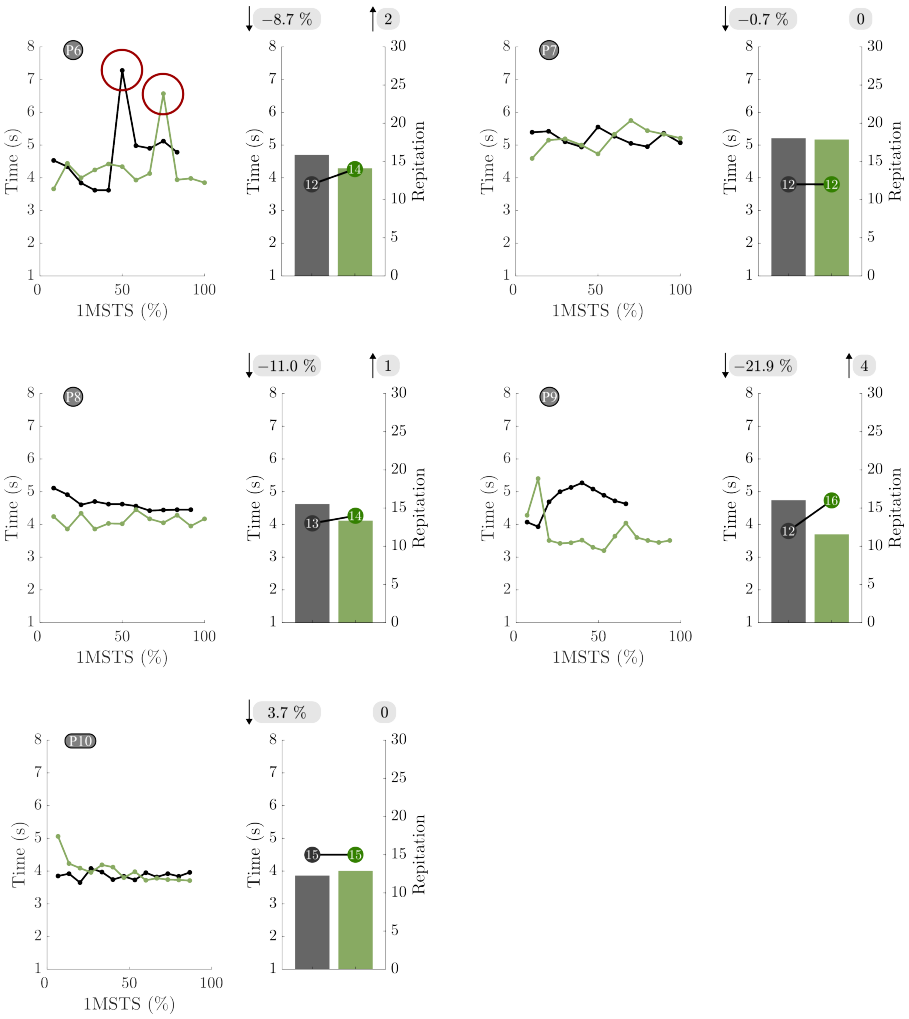


**Fig. S3 1-Minute Sit-to-Stand Test: individual sit-and-stand duration, mean duration, and total repetition under *ExoOff* and *ExoOn* conditions.** The line plot on the left for each participant shows the time duration of each sit-and-stand repetition during the 1-minute sit-to-stand test (1MSTS), with each point representing the duration of a single sit-and-stand movement. The right panel (bars) shows the mean sit-and-stand time within the 1MSTS together with the total number of repetitions (circles with numbers). Grey denotes *ExoOff* condition and green denotes *ExoOn* condition.

Among the ten older adults who performed the 1-minute sit-to-stand test (1MSTS), one participant (P1) was only able to complete a 30 s sit-to-stand test due to physical limitations and is therefore not shown in Fig. S3. For the remaining nine older participants, exosuit assistance generally improved sit-and-stand performance. Two participants completed four additional sit-and-stand cycles within 1 minute in the *ExoOn* condition compared with *ExoOff*, with their mean time per cycle reduced by 21.9% and 12.4%, respectively. Two other participants completed three additional repetitions, two completed two additional repetitions, and one completed one additional repetition, whereas the remaining two participants performed the same number of repetitions with and without assistance. In Fig. S3, red circles highlight individual sit-and-stand cycles with a sudden increase in duration, indicating brief rests taken by the older participants. For example, in participant 6 (P6), these prolonged cycles occur noticeably earlier in the *ExoOff* condition than in the *ExoOn* condition, suggesting that the exosuit assistance delays the onset of fatigue and enables more consistent sit-and-stand performance for this participant.


**Fig. S4 6-Minute Walking Test: individual metabolic cost of transport under *ExoOff* (grey) and *ExoOn* (green) conditions.** The line plot on the left illustrates the steady-state metabolic cost of transport for each participant throughout the 6-minute walking test. The bar on the right shows the corresponding mean steady-state metabolic cost.

Individual walking metabolic cost of transport information of older adults was shown in Fig. S4. Among the 10 older adults who completed the 6-minute walking test, one participant (P10) declined to wear the COSMED K5 metabolic measurement system due to discomfort with the respiratory mask; As a result, the metabolic data of P10 are unavailable and excluded from analysis. Across the remaining nine participants, 7 out of 9 (77.8%) demonstrated a reduction in metabolic cost of transport when walking with exosuit assistance compared with the *ExoOff* condition. This indicates that the exosuit delivered a beneficial metabolic effect for the majority of older adults. Two participants instead showed increased metabolic expenditure during *ExoOn*, including one with an 18% increase. These findings underscore the substantial heterogeneity in how older adults respond to exosuit mechanical assistance. The observed increases in metabolic cost may reflect limited adaptation to the exosuit, which can induce anxiety or prompt compensatory gait strategies that elevate energetic demand.

## Individual Gait Smoothness

The boxplots (Fig. S5) indicate that participants exhibited significantly ($n = 10$, $p < 0.001$) lower Spectral Arc Length (SPARC) values during walking in the *ExoOn* condition than in *ExoOff* ($2.60 \pm 0.05$, $2.43 \pm 0.04$, respectively, mean $\pm$ s.e.m.), reflecting smoother movement with assistance. In contrast, overall smoothness during the sit-and-stand was lower than during walking, likely because this task places greater demands on balance control for older adults. Marked inter-individual variability was also observed in sit-and-stand smoothness ($n = 10$, $p > 0.05$). While seven participants showed higher or comparable smoothness under *ExoOn*, three exhibited reduced smoothness with assistance. This suggests that exosuit assistance may disrupt the natural timing of the transition for some individuals, or that difficulty adapting to the device may induce anxiety, increase effort, and elicit compensatory movement strategies, ultimately reducing smoothness.

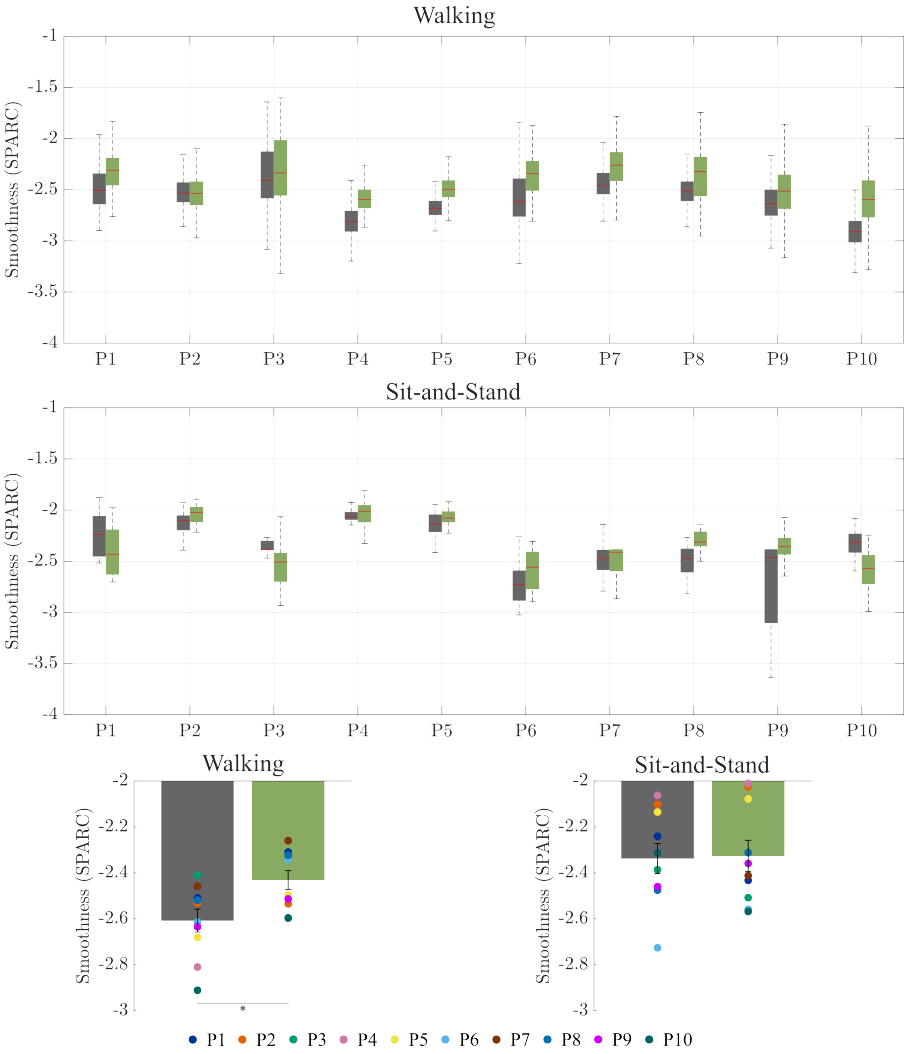


**Fig. S5 Individual and mean gait Smoothness in Spectral Arc Length (SPARC) under *ExoOff* and *ExoOn* conditions.** The central red line in each box indicates the individual median SPARC computed over all segmented steps during walking or over all sit-and-stand repetitions, and the lower and upper edges of each box represent the 25th and 75th percentiles. The bars shown below represent the mean smoothness (SPARC) across participants.

# Distribution of Sense of Agency Responses

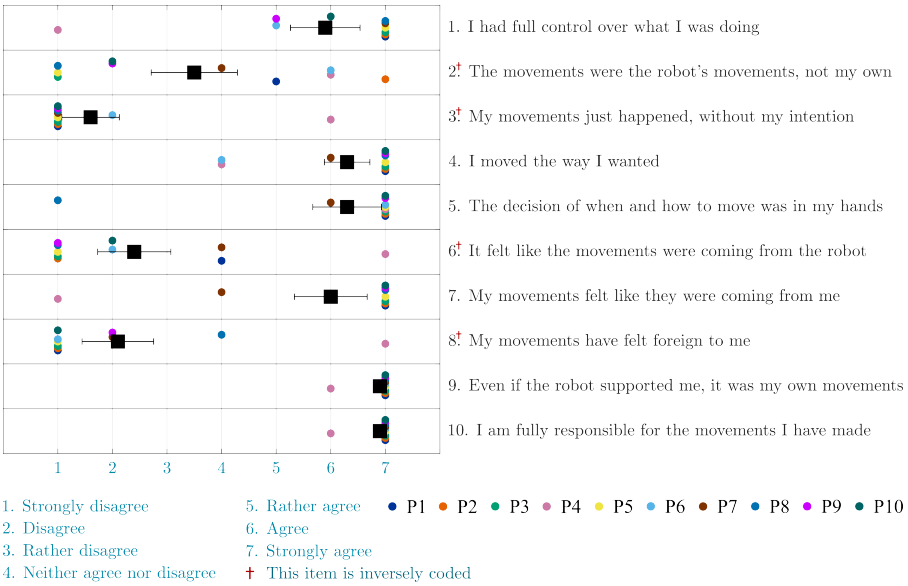


**Fig. S6 Individual and mean responses to the 10-item sense of agency questionnaire.** Participants' mean (± s.e.m.) responses to each item of the 7-point sense of agency questionnaire (ranging from "Strongly disagree" to "Strongly agree"). Y-axis represents each question, x-axis represents the Likert response option, while colored circular markers denote individual participants' responses. Items 2, 3, 6, and 8 are inversely coded, whereas items 1, 4, 5, 7, 9, and 10 follow the standard scoring direction.